НОВЫЕ МАТЕРИАЛЫ И НАНОТЕХНОЛОГИИ

MATERIAL SCIENCE AND NANOTECHNOLOGIES

doi: 10.17586/2226-1494-2022-22-1-25-32

A study of silicon *p-n* structures with mono- and multifacial photosensitive surfaces

Avazbek Mirzaalimov[1], Jasurbek Gulomov[2]✉, Rayimjon Aliev[3], Navruzbek Mirzaalimov[4], Suhrob Aliev[5]

[1,2,3,4] Andijan State University, Andijan, 170100, Uzbekistan
[5] Andijan Machine-Building Institute, Andijan, 170100, Uzbekistan

[1] avazbek.mirzaalimov@mail.ru, https://orcid.org/0000-0003-2846-1901
[2] jasurbekgulomov@yahoo.com✉, https://orcid.org/0000-0001-7516-987X
[3] alievuz@yahoo.com, https://orcid.org/0000-0003-1986-2199
[4] mirzaalimov90@mail.ru, https://orcid.org/0000-0002-9264-3710
[5] suhrob_asr89@mail.ru, https://orcid.org/0000-0002-4494-8261

Abstract
Increase in the efficiency and reduction of silicon consumption in production of solar cells are relevant problems. Designing two and three facial solar cells can be seen as a solution for such tasks. Compared to usual SC, the output power of two and three facial solar cells exceeds by 1.72 times by 2.81 times, respectively. Illumination of solar cells with high intensity light makes the temperature of its heating an important characteristic. Therefore, the paper investigates the influence of temperature on properties of multifacial solar cells. We defined the nature of change of temperature coefficients for the main photovoltaic parameters that are inherent to silicon solar cells under various (one, two and three facial) conditions of lighting. Temperature coefficients of three facial solar cells are $2.52 \cdot 10^{-3}$ V/K for open circuit voltage and $1.8 \cdot 10^{-3}$ K^{-1} for fill factor of I-V. At temperature change of SC from 300 K to 350 K, the density of short circuit current decreases only by 4 %.

Keywords
silicon, solar cell, simulation, three facial sensitivity, p-n junction, efficiency, lighting, temperature

Acknowledgements
The authors are grateful to the staff of the Renewable Energy Sources Laboratory at Andijan State University for their invaluable assistance in preparing this article.

For citation: Mirzaalimov A., Gulomov J., Aliev R., Mirzaalimov N., Aliev S. A study of silicon *p-n* structures with mono- and multifacial photosensitive surfaces. *Scientific and Technical Journal of Information Technologies, Mechanics and Optics*, 2022, vol. 22, no. 1, pp. 25–32. doi: 10.17586/2226-1494-2022-22-1-25-32

УДК 621.382

Исследование кремниевых *p-n* структур с моно- и мультифоточувствительными поверхностями

Авазбек Алишерович Мирзаалимов[1], Жасурбек Гуломов[2]✉, Раймжон Алиев[3], Наврузбек Алишер угли Мирзаалимов[4], Сухроб Алиев[5]

[1,2,3,4] Андижанский государственный университет, Андижан, 170100, Узбекистан
[5] Андижанский машиностроительный институт, Андижан, 170100, Узбекистан

[1] avazbek.mirzaalimov@mail.ru, https://orcid.org/0000-0003-2846-1901
[2] jasurbekgulomov@yahoo.com✉, https://orcid.org/0000-0001-7516-987X
[3] alievuz@yahoo.com, https://orcid.org/0000-0003-1986-2199
[4] mirzaalimov90@mail.ru, https://orcid.org/0000-0002-9264-3710
[5] suhrob_asr89@mail.ru, https://orcid.org/0000-0002-4494-8261

© Mirzaalimov A., Gulomov J., Aliev R., Mirzaalimov N., Aliev S., 2022

Аннотация

Повышение эффективности и сокращение расхода кремния при производстве солнечных элементов являются актуальными проблемами. Один из путей их решения — создание двух- и трехлицевых солнечных элементов. Выходная мощность солнечного элемента при двухстороннем освещении в 1,72 раза и при трехстороннем освещении в 2,81 раза превышает мощность односторонне освещенного (обычного) солнечного элемента. При освещении солнечного элемента светом высокой интенсивности актуальным становится учет температуры его нагрева. В работе исследовано влияние температуры на свойства многосторонне освещаемого солнечного элемента. Определен характер изменения температурных коэффициентов основных фотоэлектрических параметров кремниевых солнечных элементов при различных условиях (одно-, двух- и трехстороннего) освещения. Температурный коэффициент трехсторонне освещаемых солнечных элементов для напряжения холостого хода составил величину $2{,}52 \cdot 10^{-3}$ В/К, коэффициент заполнения вольтамперной характеристики $1{,}8 \cdot 10^{-3}$ К$^{-1}$. При изменении температуры солнечного элемента от 300 до 350 К плотность тока короткого замыкания уменьшается всего на 4 %.

Ключевые слова

кремний, солнечный элемент, моделирование, трехсторонняя чувствительность, *p-n* переход, эффективность, освещение, температура

Благодарности

Авторы выражают благодарность сотрудникам Лаборатории возобновляемых источников энергии Андижанского государственного университета за активную помощь в подготовке статьи.

Ссылка для цитирования: Мирзаалимов А.А., Гуломов Ж., Алиев Р., Мирзаалимов Н.А., Алиев С. Исследование кремниевых *p-n* структур с моно- и мультифоточувствительными поверхностями // Научно-технический вестник информационных технологий, механики и оптики. 2022. Т. 22, № 1. С. 25–32 (на англ. яз.). doi: 10.17586/2226-1494-2022-22-1-25-32

Introduction

Continuous growth of the needs in energy that humanity has stimulates faster development of renewable energy sources. They are the most primary solutions that ensure growing energy consumption without negative impact on the environment [1]. According to official information from “International Energy Agency”, the contribution of renewable energy sources (RES) in 2021 reaches up to 276 GW. The widest circulation among different types of RES has evolved from sunlight to thermal and electric energy [2]. For transformation of sunlight to electric energy, the semiconductor solar cells (SC) are generally used. More than 85 % of the produced by the industry SC are made on a silicon basis [3]. For this reason, we chose silicon SC as the main object of research. The efficiency of silicon SC that agree with theoretical expectations does not exceed 29 % [4]. But both industrial and laboratory silicon SC did not reach this value yet. Therefore, there is a need in researches on the increase in efficiency of SC and decrease in prime cost of silicon. Numerous theoretical and experimental works characterized by different scientific and technical approaches are carried out in this direction. For example, for the purpose of passivation of recombination activity and improvement of optical properties, a frontal surface of silicon SC is covered with a layer of SiN_x by 75 nanometers thick or SiO_2 by 100 nanometers thick [5]. Authors in [6] introduced nanoparticles of metals to increase the efficiency of silicon SC. For the increase in the photovoltaic transformed energy, silicon bifacial SC were designed [7]. However, in experiments, it was established that lighting the front side of the silicon bifacial SC showed the efficiency by 19.4 %, while lighting the back side of the silicon bifacial SC reached the efficiency equal to 16.5 %. In experiment, front and rear side of bifacial SC were 18.4 % and 18.1 %, respectively. So, the values for the efficiency of both sides reached symmetry [8]. In our work, the three facial silicon SC (Fig. 1), which is offered in [9], is studied for the first-time. In addition to physical mechanism of energy transformation in multifacial solar cells, influence of illumination and temperature on them has not been studied yet. For widespread introduction of any new design of SC, it is important to estimate the influence of illumination conditions and temperature changes on their photovoltaic parameters. For example, the influence of sunlight incident angle changes and temperature changes on the main photovoltaic parameters of SC on silicon base with volume metals nanoparticles was investigated in [10, 11]. Assessment of silicon SC temperature and impact of temperature changes on its photovoltaic parameters is crucial and of practical interest at three facial lighting conditions. Our work deals with the solution of this task.

If one facial solar cell is called a solar cell with monofacial photosensitive surfaces, hence two or three facial solar cells can be called solar cells with multifacial photosensitive surfaces. In the feature, solar cells with two,

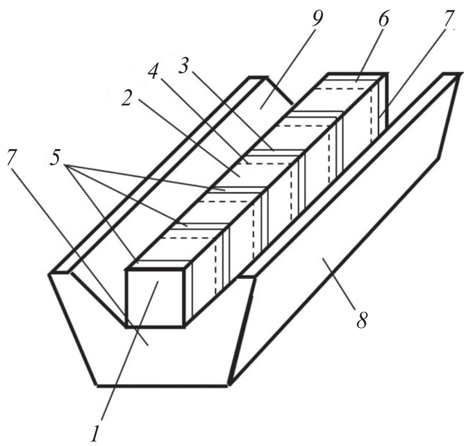

Fig. 1. Construction of a three facial solar cell: *1* — silicon in prism form; *2* — *p-n* junction; *3* — frontal contact; *4* — back contact; *5* — frontal surface; *6* — lateral face; *7* — reflector; *8* — the substrate in a tray form; *9* — silver mirror

three or four photosensitive surfaces will represent one family of multifacial solar cells.

Method

There are various research methods, for example, experimental, theoretical and modeling ones. Theoretical methods are divided into the following two groups:
1) fundamental theory of physical processes;
2) analytical solutions of the empirical equations received on experimental data.

The method of modeling is considered more difficult, as both fundamental theories and empirical formulas are used. A basis of modeling of semiconductor structures work out the private differential equations. Calculation of private differential equations in the analytical way is very laborious, therefore numerical methods are used. For the sequence of calculations by numerical methods, it is possible to create appropriate algorithms. For the solution of private differential equations, it is important to accept entry boundary conditions. Entry boundary conditions can take certain values or a form of function. When modeling physical processes as entry boundary conditions, one should use empirical formulas.

For modeling a design of SC, the simplified geometrical model is created. The geometrical model of SC with various illumination systems is given in Fig. 2. One, two and three facial solar cells depend on illumination conditions in our research. So, if only (L_B) or (L_B, L_A) or (L_B, L_A, L_C) faces are illuminated, they can be taken into account respectively as a one, two or three facial solar cells. On the front side of SC, the ray of sunlight falls perpendicularly. Flat reflectors from silver are placed on two sides of solar cells with an angle of 45 degree to ensure uniform light on all three surfaces of the solar cell. SC has a design in the form of a long prism, which width and height are identical: l = 175 μm. The base of SC represents conductivity p-type silicon with concentration of acceptor impurity $p = 10^{15}$ cm^{-3} and 171.5 μm thick, and an emitter layer of n-type of conductivity with concentration of phosphorus impurity $n = 10^{17}$ cm^{-3} and 3.5 μm thick. In the industry, silicon solar cells are made with thickness of 175 μm. If industrial silicon solar is divided into many pieces with width of 175 μm, a solar cell, which is like our geometric model, can be formed for the experiment. So, in this paper, the geometrical parameters of the cell are taken as parameters of an industrial silicon solar cell. Illumination of SC corresponds to AM1.5G range condition.

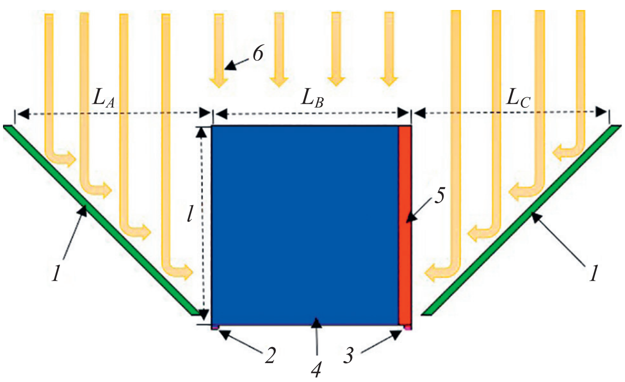

Fig. 2. Geometrical model of a three facial solar cell: *1* — silver reflector; *2* and *3* — electrodes; *4* — *p*-type silicon base; *5* — *n*-type emitter layer; *6* — sunlight beam; l — width and height (the prism basis) of a solar cell. $L_A = L_B = L_C = l$

As noted above, during the modulation of semiconductor structures, private differential equations play the main role. For example, for determination of electric parameters of semiconductor p-n structure in equilibrium conditions it is enough to use a formula for Fermi statistics:

$$n = N_c F_{1/2}\left(\frac{E_{F,n} - E_c}{kT}\right) \text{ and } p = N_V F_{1/2}\left(\frac{E_V - E_{F,p}}{kT}\right), \quad (1)$$

and a formula for Poisson's equation:

$$\Delta\varphi = -\frac{q}{\varepsilon}(p - n + N_D + N_A), \quad (2)$$

where $F_{1/2}$ is Fermi half integral; E_c is conduction band energy; E_V is valence band energy; $E_{F,n}$ is quasi fermi energy for electrons; $E_{F,p}$ is quasi fermi energy for holes; T is absolute temperature; N_c is density of states in the conduction band; N_V is density of states in valence band; k is Boltzmann constant; ε is permittivity; n and p are concentration of electrons and holes; N_D and N_A are donor and acceptor concentration; q is electron charge; φ is electric potential; Δ is Laplace operator.

Based on formula (1), it is possible to determine distribution of charge carriers concentration by semiconductor structure. Analytical function evaluation of Fermi statistics is impossible because its part is half integral Fermi. Therefore, Fermi statistics can be calculated by using Boltzmann approximation. But, Boltzmann distribution yields more exact results only at certain intervals of energy.

In this work, numerical calculation on the basis of "Sentaurus TCAD" is executed and used directly a function of Fermi statistics. Inserting the calculated concentration of electrons and holes into Poisson's equation, it is possible to define the distribution of tension or potential of the electric field in a semiconductor structure.

Modeling a semiconductor SC is considered among various instrument structures to be more difficult. It is connected with the fact that in the SC models except electric and thermal properties, it is still necessary to consider optical properties. For determination of optical properties by means of the "Sentaurus Device" tool, the transfer matrix method (TMM), ray tracing method and beam propagation method are also used. Each of the mentioned methods has its irreplaceable advantages. For example, TMM allows one to consider the interferential phenomena when calculating optical properties of the thin layer of SC. For determination of optical properties, the ray tracing method is used. When using the ray tracing method, there is an opportunity to consider the beams that fall, refract and are reflected as independent beams. Population of rays is stopped when ray energy is below the critical intensity that is defined in simulation command field. Therefore, in the modeling mode at the end of calculation, light beams are divided into parts: absorbed, free and stopped. One beam can be divided into a thousand parts.

A part of beams can be reflected from a surface, and a part can pass through, and they are considered to be free. The beam absorbed in SC loses energy and its further growth stops. The general energy falling on SC is expressed by a formula:

$$P_{total} = P_{abs} + P_{escape} + P_{stopped},$$

where P_{total} is total energy of falling beam; P_{abs} is energy of absorbed light; P_{escape} is energy of escaped light; $P_{stopped}$ is energy of stopped light.

For determination of optical properties of devices, it is necessary to know values of refraction and absorption indexes and for the materials which are contained in the structure. Optical parameters of any material are expressed as a complex index of refraction by the formula, which consists of a real and imaginary parts:

$$n_{tot}(\lambda) = n(\lambda) + ik(\lambda),$$

where n_{tot} is complex refractive index; n is real part of complex refractive index; k is imaginary part of complex refractive index; λ is wavelength.

Imaginary part of a refraction index expresses excitement coefficient. The size of both coefficients depends on light wavelength. The exact function of dependence of these coefficients for various materials is not defined. Therefore, in the modeling, table of dependencies of complex refractive index on light wavelength is used in simulation. So, accuracy and reliability of the optical properties of devices determined by way of modeling is provided.

The absorption coefficient of material is expressed through dependencies of the coefficient of excitement on wavelength in the following form:

$$\alpha(\lambda) = \frac{4\pi k}{\lambda},$$

where α is absorption coefficient.

When calculating optical properties using the Ray tracing method, certain boundary conditions are entered. The relationship between the angle of the incident, reflected and refracted beams are expressed by Snell's the law in the form:

$$\frac{n_1}{n_2} = \frac{\sin(\gamma)}{\sin(\theta)}, \ \beta = \theta,$$

where n_1 and n_2 are refractive indices of media; β is angle of incident light; γ is angle of refracted light; θ is angle of reflected light.

The relationship between energy of the falling, reflected and refracted beams are expressed by Fresnel equations:

$$\begin{cases} r_t = \dfrac{n_1\cos\beta - n_2\cos\gamma}{n_1\cos\beta + n_2\cos\gamma} \\ t_t = \dfrac{2n_1\cos\beta}{n_1\cos\beta + n_2\cos\gamma} \end{cases} \text{and} \begin{cases} r_p = \dfrac{n_1\cos\gamma - n_2\cos\beta}{n_1\cos\gamma + n_2\cos\beta} \\ t_p = \dfrac{2n_1\cos\beta}{n_2\cos\beta + n_1\cos\gamma} \end{cases},$$

where r_p, t_p, r_t and t_t are Fresnel coefficients.

When Snell's law and Fresnel coefficients are used as boundary conditions, distributions of light on the interface between two media will also depend on light wavelength. Due to the opportunities of "Sentaurus Device", the fact that values of coefficient of reflection and passing of light on border of two environments can be set by constants is important. In the real work, Snell's and Fresnel laws are used as boundary conditions for zones of contact of different environments in SC. As boundary conditions for an interval of the silver reflector and air (Fig. 2) Snell's law and constant value of coefficient of reflection $R = 1$ are adopted. It provides falling of the reflected beam perpendicularly on two lateral faces of SC without loss of energy.

The quantity of the generated electrons and holes in SC layers during the absorption of sunlight is defined by the expression for optical generation:

$$G^{opt}(x, y, z, t) = I\,(x, y, z, t)[1 - e^{-\alpha L}],$$

where G^{opt} is optical generation; I is light intensity; L is medium thickness; x, y, z are Cartesian coordinates; t is time; α is absorption coefficient of medium.

In addition to optical generation of charge carriers, our simulation also considers thermal generation. A recombination of carriers is considered to be the basis for SC accepted silicon and when modeling processes of "Auger" and "Shokley-Read-Hall". Then were calculated distribution of electrons and holes in the structure of SC by using of Fermi functions of distribution (1). Inserting a certain distribution of electrons and holes into the Poisson (2) equation, a numerical calculation is executed. For implementation of a numerical calculation, it is necessary to form plane (or volume) mesh in the structure of SC. Steps for mesh on an axis "x" from the minimum 0.04 μm to the maximum 0.08 μm, and on an axis "y" from the minimum 0.01 μm to the maximum 0.02 μm are accepted for this purpose. For the calculation of both optical and SC electric properties, we used an identical technique of formation of mesh with identical step values. During simulation, optical parameters such as absorption coefficient or absorbed photon density are calculated for a point of each optical mesh. Therefore, the ray tracing method needs optical mesh.

As a result of absorption of a photon in SC, electron-hole couples are generated which are divided by *p-n* junction and move towards contact electrodes. Change of concentration of charge carriers in a certain volume of SC on time causes the emergence of an electric current. The relationship between changes of concentration of electrons and holes over time and also the created electric current is expressed by the equation of continuity:

$$\nabla\vec{J}_n = qR_{net,n} + q\frac{\partial n}{\partial t} \ \text{and} \ -\nabla\vec{J}_p = qR_{net,p} + q\frac{\partial p}{\partial t},$$

where J_n, J_p are the current densities of electrons and holes; $R_{net,p}$, $R_{net,n}$ are the net recombination of electrons and holes; t is time; ∇ is Nabla operator.

In the "Sentaurus Device" system there are 4 models for calculating the movement of charge carriers: drift-iffusion, thermodynamic, hydrodynamic and Monte Carlo. The drift-diffusion model is a default one, and it starts automatically. In this work, for calculating the density of the current created by the directed movement of electrons and holes, we used the thermodynamic model according to the following formula:

$$J_n = -nq\mu_n(\nabla F_n + P_n\nabla T) \text{ and } J_p = -pq\mu_p(\nabla F_p + P_p\nabla T),$$

where μ_n, μ_p are the mobility of electrons and holes; F_n, F_p are the electron and hole quasi-Fermi potentials; P_n, P_p are the thermoelectric power of electrons and holes; T is absolute temperature.

The choice of this model is connected with the fact that it is necessary to consider the influence of temperature on charge transfer and formation of phonons in processes of a recombination of charge carrier. But at the same time, it is necessary to use additional calculation by the temperature equation:

$$\frac{\partial}{\partial t}(c_L T) - \nabla(k\nabla T) = -\nabla[(P_n T + F_n)\vec{J}_n + (P_p T + F_p)\vec{J}_p] - -\frac{1}{q}\left(E_c + \frac{3}{2}kT\right)(\nabla\vec{J}_n - qR_{net,n}) - -\frac{1}{q}\left(E_v + \frac{3}{2}kT\right)(-\nabla\vec{J}_p - qR_{net,n}) + \hbar\omega G^{opt}, \quad (3)$$

where k is heat conductance; c_L is heat capacity; E_c is minimum energy of conduction band; E_v is maximum energy of valence band; G^{opt} is optical generation; $R_{net,n}$ and $R_{net,p}$ are net recombination, J_n and J_p are current densities of electrons and holes; t is time; F_m is metal Fermi state; J_m is current density in metal; ω is frequency of photons; $\hbar$ is Planck constant.

In equation (3), the temperature equation is given as a non-stationary equation. But, in this paper, the stationary form of temperature equation has been used to calculate temperature of the lattice. If it is taken that temperature does not depend on the time, the time derivative of temperature, which is located the left side of equation (3), will be equal to zero. So, the equation (3) will be changed from non-stationary to its stationary form.

For the solution of equation (3), thermal boundary conditions should be applied. Thermopowers in the semiconductor and metal are various. Therefore, the thermal resistive boundary condition is calculated:

$$k\hat{n}\nabla T = \frac{T_{ext} - T}{R_{th}}, \quad (4)$$

where R_{th} is external thermal resistance; T_{ext} is external temperature; $\hat{n}$ is a unit vector in the direction of the outer normal.

If the right side of equation (4) is equal to zero, it can be used for thermally insulated interfaces. Assuming an interface between materials 1 and 2 such that $\Delta T = T_2 - T_1 > 0$, $\vec{H}_1$ is the heat flux density entering material 1 and $\vec{H}_2$ is the heat flux density leaving material 2. Hence, the thermal boundary condition at the interface between materials 1 and 2 can written as:

$$\vec{H}_1 = \vec{H}_2,$$
$$\vec{H}_1 = \frac{T_2 - T_1}{R_{d,th}}$$

where $R_{d,th}$ is the interface-distributed resistance.

In other words, it is not enough to choose the "Thermodynamic" command for the correct use of the thermodynamic model in the command file of the "Sentaurus Device" tool in the section "Physics". In addition, in the command file in the section "Solve", it is necessary to start calculation of the equation of "Thermodynamic".

Thus, according to the specified sequence of operations, the calculation of SC properties in the conditions of three facial lighting is executed.

Results and discussion

The main photovoltaic parameters of silicon SC with thickness of 175 μm are determined under 4 various conditions of lighting. The influence of temperature on the main photovoltaic parameters of SC is studied. I-V characteristic of silicon SC calculated for various conditions of lighting is given in Fig. 1. Note that the volume of a short circuit current of SC for the lighting conditions in parallel (the front side with vertical *p-n* junction) or perpendicularly (lateral face with horizontal *p-n* junction) to the front of *p-n* junction are identical. This fact means that the mechanics of photo generation and collecting of charge carriers by *p-n* junction are identical for the accepted SC sizes. Short circuit current and output power of SC have exceeded usual monofacial SC parameters by 1.72 times in bifacial lighting and by 2.81 times in three facial lighting. Open circuit voltage of SC has been greater 1.023 times in bifacial lighting and 1.047 times in three facial lighting than that of custom monofacial SC. The analysis of the known literary data demonstrated that at bifacial lighting, silicon SC can exceed short circuit current from 20.1 % to 68.1 % of parameter at its monofacial lighting [12]. It is possible to consider that the received estimated results confirmed by the known experimental data Fig. 3 shows I-V characteristics of one, two and three facial silicon solar cells at temperature of 300 K.

For determination of temperature dependencies of the main photovoltaic parameters of the silicon SC model, such I-V characteristics as shown in Fig. 3 were calculated for the temperature range from 300 K to 350 K. Each data of I-V characteristics was reworked by using new software created for calculating the photoelectric parameters from data of

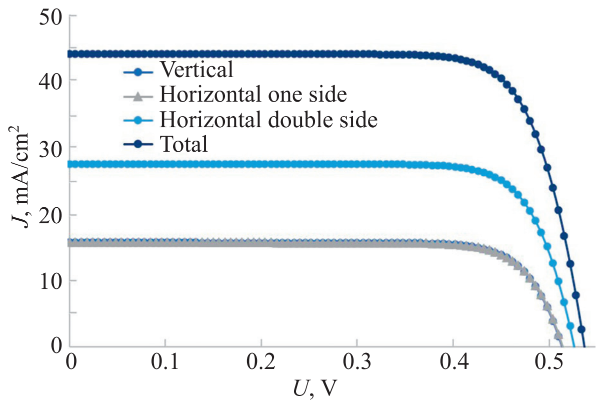

Fig. 3. I-V characteristics of silicon solar cells at various illumination conditions

I-V characteristics. So, photoelectric parameters of a solar cell were identified for the temperature range from 300 K to 350 K. The photovoltaic parameter of silicon SC that is the most sensitive to the change of temperature is open circuit voltage. For this reason, reduction of silicon SC efficiency with temperature increase can be interpreted through the change of the open circuit voltage. The contribution of processes of "Auger" recombination during the change of open circuit voltage of SC with temperature is rather high in comparison with other types of a recombination. The dependence of open circuit voltage of a silicon SC on temperature under various conditions of its illumination is given in Fig. 4, *a*. We note that for all conditions of illumination of a silicon SC, the temperature coefficient of open circuit voltage accepts identical value and makes $2.52 \cdot 10^{-3}$ V/K. Means, change of the area of lighting silicon SC has no impact on temperature coefficients of the open circuit voltage. At the same time, Tiedje experimentally determined the size for the temperature coefficient of open circuit voltage $1.36 \cdot 10^{-3}$ V/K [13]. The difference in values of certain settlement and experiments can be determined by methods, apparently, with construction features of SC and contact electrodes.

Temperature change of SC will change parameters and concentration of phonons and also the concentration of electrons and holes due to thermogeneration of charge carriers. Therefore, short circuit current has to change. Curve dependencies of short circuit current of a silicon SC on temperature are given in Fig. 4, *b* under various conditions of its lighting. Similar to data in Fig. 3, the volume of short circuit current of silicon SC when lighting it from two and three sides significantly exceeds the parameter for it during monoside lighting. Therefore, in Fig. 4, *b*, the changes from temperature of short circuit current of a silicon SC are given in relative units. At the increase in temperature of SC from 300 K to 350 K, the volume of a short circuit current of a silicon SC at horizontal monofacial lighting changes for 3.1 %, at horizontal bifacial lighting for 4.4 %, vertically monofacial lighting for 3.8 % and at three facial lighting for 4 %.

In the experimental work by He Wang, it is defined that the temperature coefficient of short circuit current of silicon SC at the conditions of bifacial lighting with an intensity 600 W/m^2 reaches $0.7 \cdot 10^{-3}$ K^{-1} [14].

Other important photovoltaic parameter of silicon SC is fill factor. Usually, consecutive resistance of silicon SC has significant effect on its fill factor volume. Dependencies on the temperature of short circuit current of a silicon SC under various conditions of its lighting are given in Fig. 4, *c*. The results demonstrated that value of temperature coefficients of fill factor of SE at three facial lighting is less by 2 %, than in the case of monofacial lighting. Some increase of the fill factor at the temperature of 330 K for SC with horizontal and vertical lighting is revealed. However, the function of temperature coefficient change for fill factor is uniform for all conditions of lighting. The value of temperature coefficient of the fill factor is $1.8 \cdot 10^{-3}$ K^{-1}. The reduction of temperature coefficient of fill factor of silicon SC with the increase of temperature is caused by the increase of a surface recombination of charge carriers.

Development of bifacial and three facial SC attracts economic interest. It is connected with the fact that output power of bifacial SC by 1.72 times and three facial SC by

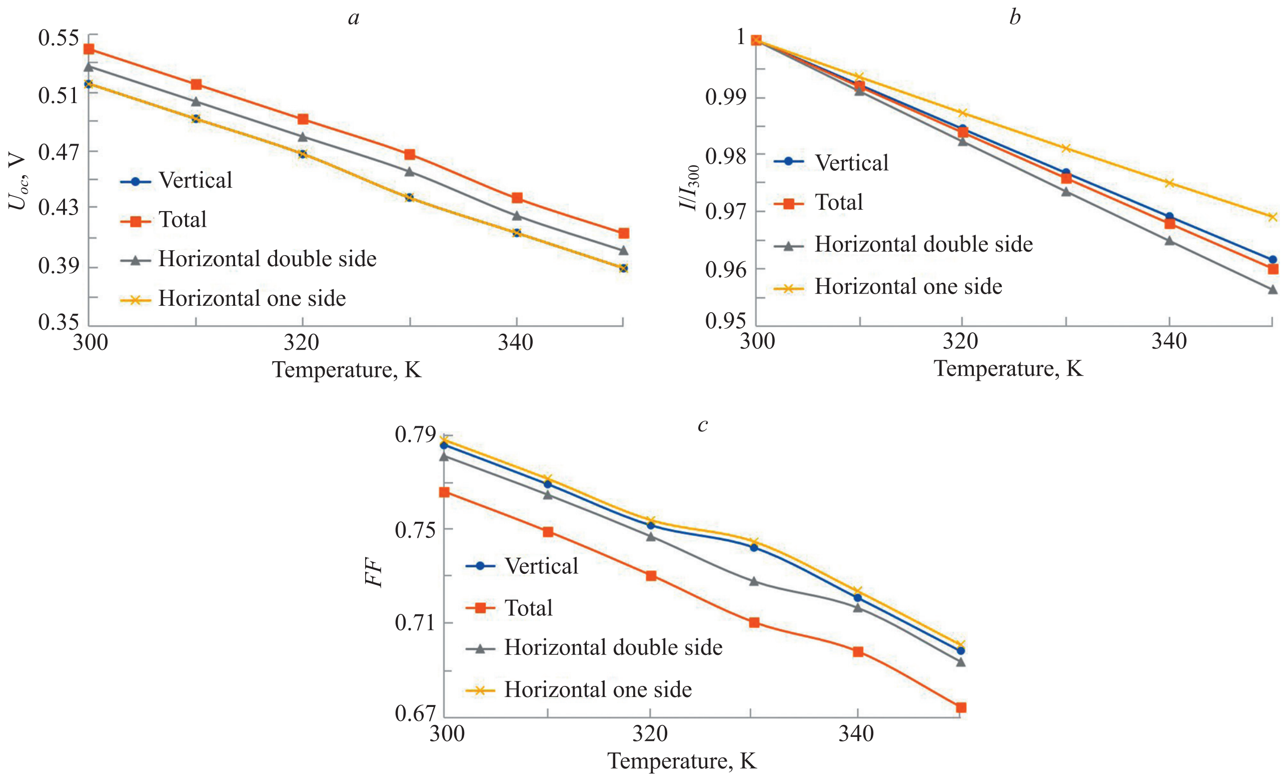

Fig. 4. Dependence on temperature of: open circuit voltage (*a*), short circuit current (*b*), fill factor (*FF*) (*c*) of a silicon solar cell under various conditions of its lighting

2.81 times exceeds the power of usual monofacial SC. By spending the single volume of silicon for the creation of three facial SC, it is possible to receive by 2.81 times more energy than in case of usual monofacial SC.

Conclusion

The quantity of the photovoltaic energy transformed by silicon SC depends on the size of its area. The increase of the area of SC causes the increase of the photons falling on its surface and, therefore, the number of the photogenerated charge carriers. Therefore, the short circuit current increases with the increase in the lighting area. Usually, the increase of open circuit voltage is insignificant under such conditions. A considerable part of photons which energy is insufficient for photogeneration of charge carriers is absorbed by silicon and other SC construction elements. It leads to heating of a body of SC, causing reduction of its efficiency. Illumination of SC with high intensity light makes the temperature of its heating an important characteristic. The nature of temperature coefficients change of the main photovoltaic parameters of silicon SC has been defined under various conditions.

Temperature coefficients for three facial SC reached $2.52 \cdot 10^{-3}$ V/K for open circuit voltage and $1.8 \cdot 10^{-3}$ K^{-1} for fill factor. Output power of SC at bifacial lighting by 1.72 times and three facial lighting by 2.81 times exceeds power usual monofacial lighting. At temperature change of SC from 300 K to 350 K, the density of short circuit current decreases by only 4 %. Comparison of material consumption for production of bifacial and three facial SC demonstrates the corresponding economy of silicon for obtaining significantly bigger photoelectric energy. Thus, it is possible to note that production and introduction of silicon SC with bifacial, three facial and multifacial lighting is expedient.

References

1. Mardani A., Jusoh A., Zavadskas E.K., Cavallaro F., Khalifah Z. Sustainable and renewable energy: An overview of the application of multiple criteria decision making techniques and approaches. *Sustainability*, 2015, vol. 7, no. 10, pp. 13947–13984. https://doi.org/10.3390/SU71013947
2. Guangul F.M., Chala G.T. Solar energy as renewable energy source: SWOT analysis. *Proc. 4th MEC International Conference on Big Data and Cmart City (ICBDSC)*, 2019, pp. 8645580. https://doi.org/10.1109/ICBDSC.2019.8645580
3. Fath P., Keller S., Winter P., Jooß W., Herbst W. Status and perspective of crystalline silicon solar cell production. *Proc. of the 34th IEEE Conference Photovoltaic Specialists*, 2009, pp. 002471–002476. https://doi.org/10.1109/PVSC.2009.5411274
4. Shockley W., Queisser H.J. Detailed balance limit of efficiency of *p-n* junction solar cells. *Journal of Applied Physics*, 1961, vol. 32, no. 3, pp. 510–519. https://doi.org/10.1063/1.1736034
5. Schmidt J., Werner F., Veith B., Zielke D., Steingrube S., Altermatt P.P., Gatz S., Dullweber T., Brendel R. Advances in the surface passivation of silicon solar cells. *Energy Procedia*, 2012, vol. 15, pp. 30–39. https://doi.org/10.1016/J.EGYPRO.2012.02.004
6. Gulomov J., Aliev R. The way of the increasing two times the efficiency of silicon solar cell. *Physics and Chemistry of Solid State*, 2021, vol. 22, no. 4, pp. 756–760. https://doi.org/10.15330/pcss.22.4.756-760
7. Hiroshi M. Radiation energy transducing device. *Patent US3278811A*. Available at: https://patents.google.com/patent/US3278811A/en (accessed: 14.09.2021).
8. Hübner A., Aberle A.G., Hezel R. Novel cost-effective bifacial silicon solar cells with 19.4% front and 18.1% rear efficiency. *Applied Physics Letters*, 1997, vol. 70, no. 8, pp. 1008–1010. https://doi.org/10.1063/1.118466
9. Aliev R., Muxtarov E., Mirzaalimov A. Quyosh generator. *Patent UZ*. № FAP00623, 2011.
10. Gulomov J., Aliev R. Numerical analysis of the effect of illumination intensity on photoelectric parameters of the silicon solar cell with various metal nanoparticles. *Nanosystems: Physics, Chemistry, Mathematics*, 2021, vol. 12, no. 5, pp. 569–574. https://doi.org/10.17586/2220-8054-2021-12-5-569-574
11. Gulomov J., Aliev R. Study of the temperature coefficient of the main photoelectric parameters of silicon solar cells with various nanoparticles. *Journal of Nano- and Electronic Physics*, 2021, vol. 13, no. 4, pp. 04033. https://doi.org/10.21272/JNEP.13(4).04033
12. Pal S., Reinders A., Saive R. Simulation of bifacial and monofacial silicon solar cell short-circuit current density under measured spectro-angular solar irradiance. *IEEE Journal of Photovoltaics*, 2020, vol. 10, no. 6, pp. 1803–1815. https://doi.org/10.1109/JPHOTOV.2020.3026141

Литература

1. Mardani A., Jusoh A., Zavadskas E.K., Cavallaro F., Khalifah Z. Sustainable and renewable energy: An overview of the application of multiple criteria decision making techniques and approaches // Sustainability. 2015. V. 7. N 10. P. 13947–13984. https://doi.org/10.3390/SU71013947
2. Guangul F.M., Chala G.T. Solar energy as renewable energy source: SWOT analysis // Proc. of the 4th MEC International Conference on Big Data and Cmart City (ICBDSC). 2019. P. 8645580 https://doi.org/10.1109/ICBDSC.2019.8645580
3. Fath P., Keller S., Winter P., Jooß W., Herbst W. Status and perspective of crystalline silicon solar cell production // Proc. of the 34th IEEE Conference Photovoltaic Specialists. 2009. P. 002471–002476. https://doi.org/10.1109/PVSC.2009.5411274
4. Shockley W., Queisser H.J. Detailed balance limit of efficiency of *p-n* junction solar cells // Journal of Applied Physics. 1961. V. 32. N 3. P. 510–519. https://doi.org/10.1063/1.1736034
5. Schmidt J., Werner F., Veith B., Zielke D., Steingrube S., Altermatt P.P., Gatz S., Dullweber T., Brendel R. Advances in the surface passivation of silicon solar cells // Energy Procedia. 2012. V. 15. P. 30–39. https://doi.org/10.1016/J.EGYPRO.2012.02.004
6. Gulomov J., Aliev R. The way of the increasing two times the efficiency of silicon solar cell // Physics and Chemistry of Solid State. 2021. V. 22. N 4. P. 756–760. https://doi.org/10.15330/pcss.22.4.756-760
7. Hiroshi M. Radiation energy transducing device. Patent US3278811A [Электронный ресурс]. URL: https://patents.google.com/patent/US3278811A/en (дата обращения: 14.09.2021).
8. Hübner A., Aberle A.G., Hezel R. Novel cost-effective bifacial silicon solar cells with 19.4% front and 18.1% rear efficiency // Applied Physics Letters. 1997. V. 70. N 8. P. 1008–1010. https://doi.org/10.1063/1.118466
9. Aliev R., Muxtarov E., Mirzaalimov A. Quyosh generator. Patent UZ. № FAP00623. 2011.
10. Gulomov J., Aliev R. Numerical analysis of the effect of illumination intensity on photoelectric parameters of the silicon solar cell with various metal nanoparticles // Наносистемы: физика, химия, математика. 2021. Т. 12. № 5. С. 569–574. https://doi.org/10.17586/2220-8054-2021-12-5-569-574
11. Gulomov J., Aliev R. Study of the temperature coefficient of the main photoelectric parameters of silicon solar cells with various nanoparticles // Journal of Nano- and Electronic Physics. 2021. V. 13. N 4. P. 04033. https://doi.org/10.21272/JNEP.13(4).04033
12. Pal S., Reinders A., Saive R. Simulation of bifacial and monofacial silicon solar cell short-circuit current density under measured spectro-angular solar irradiance // IEEE Journal of Photovoltaics. 2020. V. 10. N 6. P. 1803–1815. https://doi.org/10.1109/JPHOTOV.2020.3026141
13. Tiedje T., Engelbrecht D.A. Temperature dependence of the limiting efficiency of bifacial silicon solar cells // Proc. of the 47th IEEE

13. Tiedje T., Engelbrecht D.A. Temperature dependence of the limiting efficiency of bifacial silicon solar cells. *Proc. of the 47th IEEE Photovoltaic Specialists Conference (PVSC)*, 2020, pp. 1789–1791. https://doi.org/10.1109/PVSC45281.2020.9300921
14. Wang H., Cheng X., Yang H. Temperature coefficients and operating temperature verification for passivated emitter and rear cell bifacial silicon solar module. *IEEE Journal of Photovoltaics*, 2020, vol. 10, no. 3, pp. 729–739. https://doi.org/10.1109/JPHOTOV.2020.2974289

Photovoltaic Specialists Conference (PVSC). 2020. P. 1789–1791. https://doi.org/10.1109/PVSC45281.2020.9300921
14. Wang H., Cheng X., Yang H. Temperature coefficients and operating temperature verification for passivated emitter and rear cell bifacial silicon solar module // IEEE Journal of Photovoltaics. 2020. V. 10. N 3. P. 729–739. https://doi.org/10.1109/JPHOTOV.2020.2974289

Authors

Avazbek Mirzaalimov — PhD Student, Andijan State University, Andijan, 170100, Uzbekistan, 55807268500, https://orcid.org/0000-0003-2846-1901, avazbek.mirzaalimov@mail.ru

Jasurbek Gulomov — Student, Andijan State University, Andijan, 170100, Uzbekistan, 57221531752, https://orcid.org/0000-0001-7516-987X, jasurbekgulomov@yahoo.com

Rayimjon Aliev — D.Sc., Full Professor, Andijan State University, Andijan, 170100, Uzbekistan, 7102561277, https://orcid.org/0000-0003-1986-2199, alievuz@yahoo.com

Navruzbek Mirzaalimov — PhD Student, Andijan State University, Andijan, 170100, Uzbekistan, 57223835161, https://orcid.org/0000-0002-9264-3710, mirzaalimov90@mail.ru

Suhrob Aliev — PhD, Vice-rector, Andijan Machine-Building Institute, Andijan, 170100, Uzbekistan, 7006390145, https://orcid.org/0000-0002-4494-8261, suhrob_asr89@mail.ru

Авторы

Мирзаалимов Авазбек Алишерович — аспирант, Андижанский государственный университет, Андижан, 170100, Узбекистан, 55807268500, https://orcid.org/0000-0003-2846-1901, avazbek.mirzaalimov@mail.ru

Гуломов Жасурбек — студент, Андижанский государственный университет, Андижан, 170100, Узбекистан, 57221531752, https://orcid.org/0000-0001-7516-987X, jasurbekgulomov@yahoo.com

Алиев Райимжон — доктор технических наук, профессор, профессор, Андижанский государственный университет, Андижан, 170100, Узбекистан, 7102561277, https://orcid.org/0000-0003-1986-2199, alievuz@yahoo.com

Мирзаалимов Наврузбек Алишер угли — аспирант, Андижанский государственный университет, Андижан, 170100, Узбекистан, 57223835161, https://orcid.org/0000-0002-9264-3710, mirzaalimov90@mail.ru

Алиев Сухроб — PhD, проректор, Андижанский машиностроительный институт, Андижан, 170100, Узбекистан, 7006390145, https://orcid.org/0000-0002-4494-8261, suhrob_asr89@mail.ru

Received 30.10.2021
Approved after reviewing 10.12.2021
Accepted 31.01.2022

Статья поступила в редакцию 30.10.2021
Одобрена после рецензирования 10.12.2021
Принята к печати 31.01.2022

Работа доступна по лицензии
Creative Commons
«Attribution-NonCommercial»